THE UNIVERSITY OF READING

Fluctuation Distribution Schemes on Adjustable Meshes for Scalar Hyperbolic Equations

by

M.J. Baines & S.J. Leary

Numerical Analysis Report 6/98

DEPARTMENT OF MATHEMATICS

Fluctuation Distribution Schemes on Adjustable Meshes for Scalar Hyperbolic Equations

M.J.Baines and S.J.Leary
Department of Mathematics
University of Reading
P O Box 220, Reading, RG6 6AX, UK

Abstract

A problem with the convergence of fluctuation distribution schemes for steady hyperbolic equations on unstructured triangular meshes is that the fluctuations are not driven to zero.

One way of dealing with the problem is to allow the mesh to adjust, using the extra degrees of freedom to counteract the difficulty and improve the approximation. The method then becomes an approximate method of characteristics.

Iterative procedures for the solution of the resulting coupled equations are discussed, including steepest descent least squares and a procedure coupling least squares with multidimensional upwinding. An upwind least squares method is also proposed.

1 Introduction

Roe [1] was the first to suggest the fluctuation-distribution framework for the approximate solution of steady first order hyperbolic PDEs in multi-dimensions. In this approach nonzero *fluctuations,* or residuals, on cells are distributed by *signals*, implemented by adding weighted fractions of the fluctuations to the values of the solution at the corners of the cell. The cumulative update to the solution at a node is of the sum of the weighted contributions from all cells with that node as target.

The steps of the procedure are carried out repeatedly, updating the solution values until the total increments at every node become zero, at which point the process is said to have converged. However, for many types of discretisation, even though the total increments at a node are zero, the individual cell fluctuations do not vanish but only their weighted sums. So even at convergence the fluctuation in a cell, and hence the PDE residual, is not zero, leading to an unsatisfactory solution.

One way to alleviate the difficulty is to increase the number of degrees of freedom available by including the mesh locations as additional variables [2],[3],[4],[5]. As a consequence, when the total increments become zero the individual fluctuations in a cell are closer to zero and give a much better approximation to the PDE. The approach then resembles an approximate method of characteristics.

In this paper we shall consider a steady scalar hyperbolic scalar equation on an unstructured triangular mesh for which this situation occurs.

2 Fluctuations

The scalar conservation law

$$div \underline{F} = 0 \tag{2.1}$$

with $\underline{F} = u\underline{a}$ becomes

$$div\,(u\underline{a}) = 0, \tag{2.2}$$

equivalent to the integral form

$$\oint_S u\underline{a}.\underline{\hat{n}} dS = 0, \tag{2.3}$$

where $\underline{\hat{n}}$ is the inward unit normal to the arbitrary closed surface S in a domain Ω, say. Taking the velocity field $\underline{a}$ to be divergence-free, equation (2.2) reduces to the advection equation

$$\underline{a}.\nabla u = 0. \tag{2.4}$$

Let the domain in which equation (2.4) holds be divided into cells and let u be approximated in each cell by a finite-dimensional function U. Then on each cell we may define the fluctuation to be

$$\phi = -\int \underline{a}.\nabla U d\Omega \tag{2.5}$$

Figure 1: The normals.

(see [1],[2]) which is the integral of the residual error incurred in replacing u by U in equation (2.4).

Consider now the two-dimensional domain Ω which is the union of triangular cells T_e and let U be linear in each triangle of the form

$$U = \sum_{ei} U_{ei}\psi_{ei}(\underline{x}) \tag{2.6}$$

where the $\psi_{ei}(\underline{x})$ are linear basis functions and the suffix ei refers to the corners of the triangle. Then from equation (2.5) the fluctuation in triangle T_e is

$$\phi_e = -\int_{T_e} \underline{a}.\nabla U d\Omega = -\int_{T_e} \underline{a}.\nabla \left(\sum_{ei} U_{ei}\psi_{ei}(\underline{x}) \right) d\Omega \tag{2.7}$$

$$= -\sum_{ei} U_{ei} \int_{T_e} \underline{a}.\nabla \left(\psi_{ei}(\underline{x})\right) d\Omega \tag{2.8}$$

which may be written

$$\phi_e = \sum_{ei} k_{ei}U_{ei} \tag{2.9}$$

where

$$k_{ei} = -\int_{T_e} \underline{a}.\nabla \left(\psi_{ei}(\underline{x})\right) d\Omega = -\frac{1}{2}\underline{a}_e.\underline{n}_{ei}, \tag{2.10}$$

$\underline{n}_{ei}$ being the inward normal to the side of the triangle e opposite node i multiplied by the length of that side (see fig.1).

The vector $\underline{a}_e$ is the average field velocity

$$\underline{a}_e = \frac{1}{S_e}\int_{T_e} \underline{a} d\Omega \tag{2.11}$$

where S_e is the area of the triangle T_e.

In equation (2.10) the coefficients k_{ei} depend on $\underline{a}_e$ and the mesh coordinates. However, since

$$\sum_{ei} \psi_{ei}(\underline{x}) = 1 \tag{2.12}$$

we may deduce from equation (2.10) that

$$\sum_{ei} k_{ei} = 0. \tag{2.13}$$

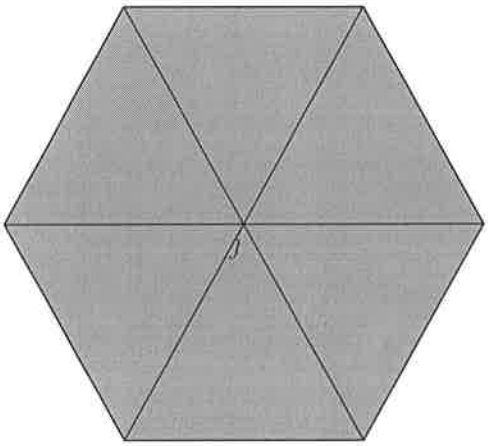

Figure 2: A patch of triangles T_j (shaded) surrounding node j.

Suppose that the suffix eI denote inflow nodes and from now on reserve the suffix ei for non-inflow nodes. Then equation (2.9) may be written

$$\phi_e = \sum_{ei} k_{ei} U_{ei} + \sum_{eI} k_{eI} U_{eI}, \tag{2.14}$$

where the U_{eI} are prescribed by the inflow conditions.

3 Signals

Define $\{T_j\}$ to be the set of triangles surrounding node j (see fig 2). In the fluctuation-signal algorithm each ϕ_e is calculated from equation (2.14) and added to the value of U_j at node j with predetermined weights w_{je}. The cumulative signal or total update at node j is then

$$\delta U_j = \sum_{\{T_j\}} w_{je} \phi_e, \tag{3.1}$$

i.e. using equation (2.14),

$$\delta U_j = \sum_{\{T_j\}} w_{je} \left(\sum_{ei} k_{ei} U_{ei} + \sum_{eI} k_{eI} U_{eI} \right). \tag{3.2}$$

The procedure may be repeated until convergence, in which case $\delta U_j = 0$ and the U values satisfy

$$\sum_{\{T_j\}} w_{je} \left(\sum_{ei} k_{ei} U_{ei} + \sum_{eI} k_{eI} U_{eI} \right) = 0. \tag{3.3}$$

We refer to three examples of weights w_{je}. First, suppose that the weights w_{je} arise from a least squares minimisation of ϕ over the whole domain (see [2]). Then the weights are proportional to the k_{je} and their sum is zero by equation (2.13). The method is non-conservative in the usual sense, but the main advantage is the existence of the least squares functional which can be used as a monitor to measure convergence and in designing iterative procedures for reaching the solution. Secondly, let the constant fraction one-third be added to a multiple of the least squares weights, giving a two-dimensional Lax-Wendroff scheme [6]. The sum of the weights is now unity, enforcing conservation, and the method is second-order accurate, but there is no objective functional. In the third example the weights are those associated with the PSI method of Multidimensional Upwinding [6],[7], which is a conservative positive upwind scheme. In this scheme the weights are all non-negative but are solution-dependent in general.

4 Null Space

Equation (2.14) may be written in the matrix-vector form

$$\mathbf{\Phi} = K\mathbf{U} + K_I \mathbf{U}_I \tag{4.1}$$

where $\mathbf{\Phi}$ and $\mathbf{U}$ are vectors of the values of ϕ_e and U_j taken over all cells and nodes, respectively. The function U is assumed to be continuous and the matrices K, K_I are therefore assembled matrices containing combinations of the coefficients k_{ei} as elements. Equation (3.1) may now be written in the matrix-vector form

$$\delta\mathbf{U} = W\mathbf{\Phi} \tag{4.2}$$

where W is the matrix of weights w_{ei}. From equation (4.1)

$$\delta\mathbf{U} = W\left(K\mathbf{U} + K_I\mathbf{U}_I\right). \tag{4.3}$$

At convergence equation (4.2) gives

$$W\mathbf{\Phi} = 0 \tag{4.4}$$

while from (4.3) $\mathbf{U}$ satisfies the matrix equation

$$WK\mathbf{U} = -WK_I\mathbf{U}_I. \tag{4.5}$$

Convergence of the fluctuation-signal approach is equivalent to solving the (possibly nonlinear) equation (4.5) for $\mathbf{U}$ (corresponding to $\delta\mathbf{U} = \mathbf{0}$). However, from equation (4.4), unless the matrix W is square and nonsingular $\delta\mathbf{U} = \mathbf{0}$ does not imply that $\mathbf{\Phi} = 0$.

The three examples quoted in the previous section have matrix forms characterised as follows. Least squares minimisation of $\mathbf{\Phi}$, which results in weights proportional to k_{je}, corresponds to $W = K^t$ and equation (4.5) becomes

$$K^tK\mathbf{U} = -K^tK_I\mathbf{U}_I \tag{4.6}$$

while equation (4.4) becomes $K^t\mathbf{\Phi} = 0$ so that $\mathbf{\Phi}$ lies in the null space of K^t. The Lax-Wendroff method corresponds to $W = \frac{1}{3}I + \alpha K^t$ where α is a constant: $\mathbf{\Phi}$ lies in the null space of $\frac{1}{3}I + \alpha K^t$. For the PSI method W depends on $\mathbf{U}$ but is ≥ 0: the null space cannot include vectors with only positive components (unlike the previous two methods).

We now describe a simple configuration in which this situation arises. Let the domain be the unit square with $n+1$ nodes along each side. The interior of the square is discretised with $2n^2$ triangular cells and $(n+1)^2$ nodes by dividing each square of a uniform grid by a constantly orientated diagonal (see fig.3). Suppose further that there are just two inflow sides so that the number of non-inflow nodes is n^2. Then the dimensions of the vectors $\mathbf{\Phi}$ and $\mathbf{U}$ are $2n^2$ and n^2 respectively, while those of the matrices K and W are $2n^2 \times n^2$ and $n^2 \times 2n^2$. It follows that the matrix W possesses a null space of dimension n^2 and that at convergence equation (4.4) merely tells us that $\mathbf{\Phi}$ belongs to that null space. For example, if the weights in equation (3.1) sum to zero then any row of W has a zero sum and the vector $\mathbf{\Phi} = (1, 1, ..., 1)$ lies in the null space of W.

In general W will always possess a null space and as a result $\delta\mathbf{U} = \mathbf{0}$ will not automatically imply that $\mathbf{\Phi}$ is small.

5 Adjustable Nodes

One way of tackling the problem of the null space is to increase the number of degrees of freedom by regarding the mesh locations as additional variables, in

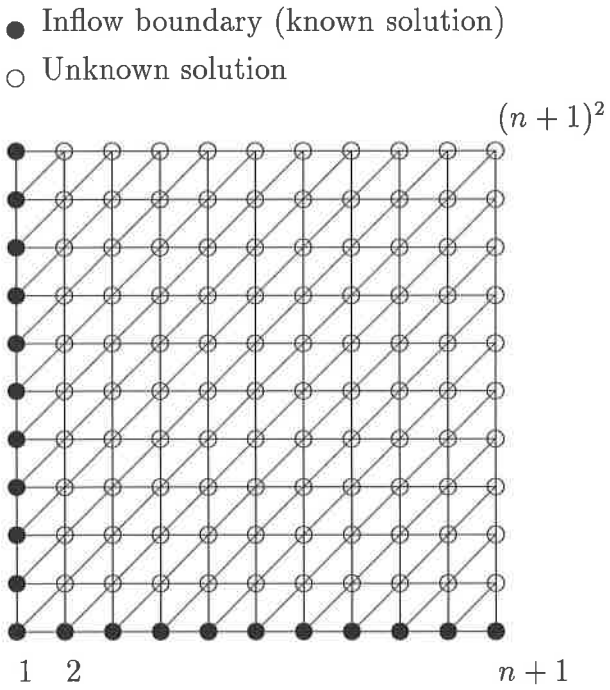

Figure 3: A square domain with $2n^2$ triangular cells and n^2 unknowns.

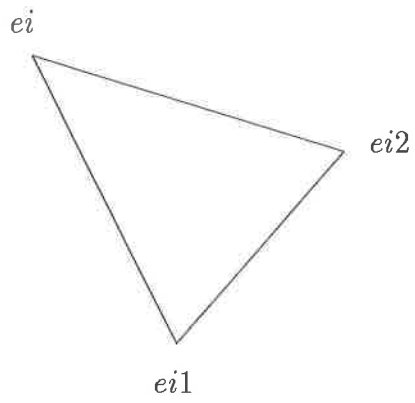

Figure 4: A patch of triangles T_j (shaded) surrounding node j.

a way similar to that exploited elsewhere [3],[4],[5]. A natural construction in the present context is to use the fluctuations to generate signals for adjusting the mesh as well as the solution and this can be implemented as follows.

5.1 Fluctuations

First we derive a nodal based form of the fluctuation (2.9), which may be obtained by writing

$$\phi_e = \sum_{ei} k_{ei} U_{ei} = -\frac{1}{2} \sum_{ei} U_{ei} \underline{a}_e . \underline{n}_{ei} \tag{5.1}$$

$$= -\frac{1}{2} \sum_{ei} U_{ei} \underline{a}_e . \left(-(Y_{ei2} - Y_{ei1}) \underline{i} + (X_{ei2} - X_{ei1}) \underline{j} \right) \tag{5.2}$$

where $\underline{i}$,$\underline{j}$ are unit vectors in the x, y directions and $ei1, ei2$ are the vertices of T_e taken anticlockwise from ei (fig 3). Writing $\underline{a}_e = (a_e, b_e)$, (5.2) becomes

$$\frac{1}{2} \sum_{ei} U_{ei} \left((Y_{ei2} - Y_{ei1}) a_e - (X_{ei2} - X_{ei1}) b_e \right) \tag{5.3}$$

$$= \frac{1}{2} \sum_{ei} \left(-Y_{ei} (U_{ei2} - U_{ei1}) a_e + X_{ei} (U_{ei2} - U_{ei1}) b_e \right) \tag{5.4}$$

so that an alternative form of ϕ_e is ([8])

$$\phi_e = \sum_{ei} \underline{l}_{ei} \cdot \underline{X}_{ei} \tag{5.5}$$

(cf. (2.10)), where

$$\underline{l}_{ei} = \frac{1}{2} \Delta U_{ei} \begin{pmatrix} b_e \\ -a_e \end{pmatrix} \tag{5.6}$$

(cf. (2.12)), and $\Delta U_{ei} = U_{ei2} - U_{ei1}$ is the difference in the U values across the side opposite corner ei, taken anticlockwise around the triangle (see fig 4). Clearly

$$\sum_{ei} \underline{l}_{ei} = 0. \tag{5.7}$$

As in equation (2.14), separating out the inflow points leads to the form

$$\phi_e = \sum_{ei} \underline{l}_{ei} \cdot \underline{X}_{ei} + \sum_{eI} \underline{l}_{eI} \cdot \underline{X}_{eI}. \tag{5.8}$$

Inflow nodes are separated out here on the grounds that the $\underline{X}_{eI}$ coordinates will also naturally be partially prescribed at inflow. In some problems the $\underline{X}_{ei}$ may also be prescribed at *outflow* in order to constrain the nodes to remain on the physical boundaries of the domain.

5.2 Signals

Nodal positions may now be updated by signals in the same way as for U. Denoting the weights for these signals by $\underline{\gamma}_{je}$ the analogue to equation (3.1) is

$$\delta \underline{X}_j = \sum_{\{T_j\}} \underline{\gamma}_{je} \phi_e = \sum_{\{T_j\}} \underline{\gamma}_{je} \left(\sum_{ei} \underline{l}_{ei} \cdot \underline{X}_{ei} + \sum_{eI} \underline{l}_{eI} \cdot \underline{X}_{eI} \right). \tag{5.9}$$

At convergence

$$\sum_{\{T_j\}} \underline{\gamma}_{je} \left(\sum_{ei} \underline{l}_{ei} \cdot \underline{X}_{ei} + \sum_{eI} \underline{l}_{eI} \cdot \underline{X}_{eI} \right) = 0 \tag{5.10}$$

(cf. (3.3)).

If the weights are derived from a least squares approach they are, as in the case of U updates, proportional to $\underline{l}_{je}$.

5.3 Null Space

In matrix-vector form equation (5.8) may be written as

$$\mathbf{\Phi} = \underline{L}.\underline{\mathbf{X}} + \underline{L_I}.\underline{\mathbf{X}_I} \tag{5.11}$$

where $\underline{\mathbf{X}}$ is a vector of all the 2-vectors $\underline{X_j}$ taken over the nodes. The piecewise linear function X is assumed to be continuous and the matrices $\underline{L}$,$\underline{L_I}$ are therefore assembled matrices containing combinations of the coefficients $\underline{l_{ei}}$ as elements.

If $\underline{\Gamma}$ is defined to be the matrix of weights $\underline{\gamma_{je}}$, the matrix-vector forms of equations (5.9) and (5.10) are

$$\delta\underline{\mathbf{X}} = \underline{\Gamma}\mathbf{\Phi} = \underline{\Gamma}\,(\underline{L}\underline{\mathbf{X}} + \underline{L_I}\underline{\mathbf{X}_I}) \tag{5.12}$$

and

$$\underline{\Gamma L}\underline{\mathbf{X}} = -\underline{\Gamma L_I}\underline{\mathbf{X}_I}. \tag{5.13}$$

In the least squares method $\underline{\Gamma}$ is proportional to $\underline{L^t}$ and equation (5.13) becomes

$$\underline{L^t L}\underline{\mathbf{X}} = -\underline{L^t L_I}\underline{\mathbf{X}_I} \tag{5.14}$$

(cf. (4.6)).

Considering again the illustration of a square domain with two inflow sides discussed in the previous section, the vector $\underline{\mathbf{X}}$ will have dimension $2n^2$ and both matrices $\underline{L}$ and $\underline{\Gamma}$ have dimensions $2n^2 \times 2n^2$. Hence $\underline{\Gamma}$ is square and provided that it is non-singular, $\delta\underline{\mathbf{X}}= \mathbf{0}$ implies that $\mathbf{\Phi} = 0$, as desired.

One way to understand the situation is as follows. For a given solution U, by adjusting $\mathbf{X}$ we may construct an approximate "characteristic mesh" as a triangulation of points which lie on the characteristics of the equation (2.4). On the resulting mesh a piecewise linear approximation to U on each characteristic is approximately constant and therefore within each triangle

$$\underline{a}.\nabla U = 0 \tag{5.15}$$

giving a zero $\mathbf{\Phi}$.

However such an approximate triangulation is far from unique and it is clear that the equation

$$\phi_{ei} = \sum_{ei} \underline{l_{ei}}.\underline{X_{ei}} = 0 \tag{5.16}$$

does not uniquely determine $\underline{\mathbf{X}}$.

6 Constrained Nodal Movement

The above analysis of the situation is still valid when the nodal coordinates are constrained to move perpendicular to the approximate characteristics which suggests that we may achieve the same result when only one of the nodal coordinates is allowed to vary. A single varying nodal coordinate combined with variable U is still sufficient to allow (a) the sides of the triangles to align with the characteristics and (b) U to become constant along them: equation (5.15) holds and $\mathbf{\Phi}_e$ vanishes as required.

Suppose then that $\underline{X}_j$ is constrained to move only in a chosen direction $\underline{\widehat{N}}_j$ and denote the corresponding coordinate by N_j. We may take $\underline{\widehat{N}}_j$ to be in the direction perpendicular to the characteristic velocity field $\underline{a}_j$ at node j. Then equation (5.9) reduces to

$$\delta N_j = \sum_{\{T_j\}} \tilde{\gamma}_{ei}\phi_e = \sum_{\{T_j\}} \tilde{\gamma}_{ei}\left(\sum_{ei} \tilde{l}_{ei}N_e + \sum_{eI} \tilde{l}_{eI}N_e\right) \tag{6.1}$$

where $\tilde{\gamma}_{je} = \underline{\widehat{N}}_j.\underline{\gamma}_{je}$ and $\tilde{l}_{ei} = \underline{\widehat{N}}_e.\underline{l}_{ei}$ with $\underline{\widehat{N}}_e$ perpendicular to $\underline{a}_e$, which at convergence becomes

$$\sum_{\{T_j\}} \tilde{\gamma}_{je}\left(\sum_{ei} \tilde{l}_{ei}N_e + \sum_{eI} \tilde{l}_{eI}N_e\right) = 0. \tag{6.2}$$

Note that as in equation (5.7)

$$\sum \tilde{l}_{ei} = 0. \tag{6.3}$$

The matrix-vector equation (5.12) then becomes

$$\delta\mathbf{N} = \tilde{\Gamma}\mathbf{\Phi} = \tilde{\Gamma}\left(\tilde{L}\mathbf{N} + \tilde{L}_I\mathbf{N}_I\right) \tag{6.4}$$

where $\tilde{L}, \tilde{L}_I$ are matrices of the coefficients $\tilde{l}_{ei}, \tilde{l}_{eI}$ and $\tilde{\Gamma}$ contains the coefficients $\tilde{\gamma}_{je}$. At convergence

$$\tilde{\Gamma}\mathbf{\Phi} = 0, \qquad \tilde{\Gamma}\tilde{L}\mathbf{N} = -\tilde{\Gamma}\tilde{L}_I\mathbf{N}_I. \tag{6.5}$$

In the least squares case $\tilde{\Gamma}$ is proportional to $\tilde{L}^t$ and equation (6.5) becomes

$$\tilde{L}^t\tilde{L}\underline{\mathbf{N}} = -\tilde{L}^t\tilde{L}_I\underline{\mathbf{N}}_I. \tag{6.6}$$

7 Coupled Solutions

In the earlier illustration of simple advection across a square domain (see fig 3)the vector $\mathbf{N}$ is of dimension n^2 and the matrices L and $\tilde{\Gamma}$ now have dimensions $2n^2 \times n^2$ and $n^2 \times 2n^2$, respectively. By itself equation (6.4) has the same drawbacks as equation (4.3) with $\tilde{\Gamma}$ possessing a null space and $\delta\mathbf{N} = 0$ not implying $\mathbf{\Phi} = 0$. However, taken together with equation (4.3) we obtain at convergence the square systems

$$\begin{pmatrix} W \\ \tilde{\Gamma} \end{pmatrix} \mathbf{\Phi} = 0 \tag{7.1}$$

for $\mathbf{\Phi}$ and

$$\begin{pmatrix} WK & 0 \\ 0 & \tilde{\Gamma}\tilde{L} \end{pmatrix} \begin{pmatrix} \mathbf{U} \\ \mathbf{N} \end{pmatrix} = - \begin{pmatrix} WK_I & 0 \\ 0 & \tilde{\Gamma}\tilde{L}_I \end{pmatrix} \begin{pmatrix} \mathbf{U}_I \\ \mathbf{N}_I \end{pmatrix} \tag{7.2}$$

for $\mathbf{U}$ and $\mathbf{N}$. Provided that the left hand side matrices are non-singular we can always solve for a pair $\mathbf{U}$, $\mathbf{N}$ for which $\mathbf{\Phi} = 0$.

In three dimensions a similar argument shows that the inclusion of *two* nodal coordinates (rather than the full three available) gives rise to a square system and hence, given nonsingularity, to vanishing $\mathbf{\Phi}$ at convergence, which again accords with the method of characteristics. Indeed, in d dimensions using simplexes, the number of variable nodal coordinates to be included should be $d - 1$.

We consider some examples.

7.1 Least Squares Weights

If the fluctuation distribution scheme is derived from a least-squares minimisation of $\mathbf{\Phi}$ over both $\mathbf{U}$ and $\mathbf{N}$, the weights in W are proportional to k_{je} as before while those in $\tilde{\Gamma}$ are now proportional to

$$\tilde{l}_{je} = \widehat{\underline{N}}_j . \underline{l}_{je} = \frac{1}{2} \Delta U_{je} (a_j a_{je} + b_j b_{je}) / (a_j^2 + b_j^2)^{1/2} = \frac{1}{2} \left| \underline{a} \right| \Delta U_{je} \tag{7.3}$$

for a constant velocity field $\underline{a}$ (see equation (6.1)).

A necessary condition for nonsingularity in equation (7.1) is that the null spaces of W and $\tilde{\Gamma}$ be disjoint. However, from equations (2.13) and (6.3), the vector $\mathbf{\Phi} = (1, 1, ..., 1)$ lies in both of these null spaces, so in this special case we have not elminated the null space entirely.

Nevertheless the fact that $\mathbf{\Phi}$ is small on an approximate characteristic mesh ensures a good solution to the differential equation when $\|\mathbf{\Phi}\|_2$ is minimised. Even though the null space may not have been totally eradicated, all the $\mathbf{\Phi}$ components (including those in the null space) are small. Moreover this argument still holds when the least squares minimisation is taken over nodal coordinates alone: given any consistent weights for $\mathbf{U}$, including those possessing a null space, least squares minimisation of $\|\mathbf{\Phi}\|_2$ over $\mathbf{X}$ (or $\mathbf{N}$) alone still ensures that the effect of the null space is nullified.

We therefore may either

- choose a unified least squares minimisation of $\|\mathbf{\Phi}\|_2$ over $\mathbf{U}$ and $\mathbf{X}$ (or $\mathbf{N}$), leading to a method with an objective functional that can be monitored, *or*
- choose a least squares minimisation of $\|\mathbf{\Phi}\|_2$ over $\mathbf{X}$ (or $\mathbf{N}$) alone, combined with some other choice of weights W for $\mathbf{U}$ with other properties but lacking an objective functional. In the examples cited earlier the Lax-Wendroff or PSI schemes can be incorporated with the latter option.

We have already cited the former, unified least squares, method as an example in the text. We shall discuss the latter approach in Section 10 and also extend the idea to an upwind least squares procedure.

8 Iterative Solution Methods

We now consider iterative methods for the solution of equation (7.2) for $\mathbf{U}$ and $\mathbf{N}$. Since K depends upon $\mathbf{N}$ and L depends upon $\mathbf{U}$ in general, the two component equations in (7.2) are coupled. However, if $\mathbf{U}$ and $\mathbf{N}$ are frozen in WK, the set of equations (4.5) form a sparse linear system for $\mathbf{U}$. Similarly, if $\mathbf{N}$ and $\mathbf{U}$ are frozen in $\widetilde{\Gamma}L$, the equations (6.5) form a sparse linear system for $\mathbf{N}$. This linearisation suggests an iterative solution procedure in which steps for equation (4.5) are alternated with those for equation (6.5).

8.1 A Jacobi Iteration

For example, the relaxed Jacobi method for the independent solutions of the linearised equations (4.5) and (6.5) is

$$diag(WK)\delta\mathbf{U} = -\tau W\mathbf{\Phi} = -\tau\left(WK\mathbf{U} + WK_I\mathbf{U}_I\right) \tag{8.1}$$

and

$$diag(\tilde{\Gamma}\tilde{L})\delta\mathbf{N} = -\sigma\tilde{\Gamma}\mathbf{\Phi} = -\sigma\left(\tilde{\Gamma}\tilde{L}\mathbf{N} + \tilde{\Gamma}\tilde{L}_I\mathbf{N}_I\right), \tag{8.2}$$

where τ and σ are positive relaxation factors. In component form, for each non-inflow node j these equations (excluding inflow terms) read

$$\left(\sum_{\{T_j\}} w_{je}k_{ej}\right)\delta U_j = -\tau\left(\left(\sum_{\{T_j\}} w_{je}k_{ej}\right)U_j + \sum_{\{T_j\}} w_{je}\sum_{ei} k_{ei}U_{ei}\right) \tag{8.3}$$

using equation (2.13) and

$$\left(\sum_{\{T_j\}} \tilde{\gamma}_{je}\tilde{l}_{ej}\right)\delta N_j = -\sigma\left(\left(\sum_{\{T_j\}} \tilde{\gamma}_{je}\tilde{l}_{ej}\right)N_j + \sum_{\{T_j\}} \tilde{\gamma}_{je}\sum_{ei} \tilde{l}_{ei}N_{ei}\right) \tag{8.4}$$

using equation (5.7), denoting by ei the index of those nonzero terms in the j'th equation of equation (3.3) which are different from j. In the iterations described here we may interleave these two linearised steps.

8.2 Steepest Descent Methods

In the case of a unified L_2 minimisation of the norm of $\mathbf{\Phi}$ we may construct iterative algorithms directly using the techniques of optimisation. For example, steepest descent methods applied to the least squares equations (4.6) and (6.5) generate the iterations

$$\delta\mathbf{U} = -\tau' K^t(K\mathbf{U} + K_I\mathbf{U}_I) \tag{8.5}$$

and

$$\delta\mathbf{N} = -\sigma'\tilde{L}^t(\tilde{L}\mathbf{N} + \tilde{L}_I\mathbf{N}_I) \tag{8.6}$$

where τ',σ' are relaxation coefficients. Optimal choices of τ' and σ' consistent with the linearisation are

$$\tau' = -\frac{\mathbf{R}^t\mathbf{R}}{\mathbf{R}^t K^t K\mathbf{R}} \qquad \sigma' = -\frac{\mathbf{S}^t\mathbf{S}}{\mathbf{S}^t\tilde{L}^t\tilde{L}\mathbf{S}} \tag{8.7}$$

where

$$\mathbf{R} = K^t(K\mathbf{U} + K_I\mathbf{U}_I) \tag{8.8}$$

and

$$\mathbf{S} = \tilde{L}^t(\tilde{L}\mathbf{N} + \tilde{L}_I\mathbf{N}_I) \tag{8.9}$$

are the residuals associated with the normal equations (4.6) and (6.5).

Equations (8.5) and (8.6) are identical with the relaxed Jacobi iterations (8.3) and (8.4) under the choices

$$\tau = \tau' \sum_{\{T_j\}} k_{ei}^2 \qquad \sigma = \sigma' \sum_{\{T_j\}} \tilde{l}_{ei}^2 \tag{8.10}$$

and may be rewritten, using equations (2.13) and (6.3), as

$$\delta U_j = \frac{\sum_{\{T_j\}} k_{je} \left(\sum_{ei} k_{ei} \left(U_{ei} - U_j \right) \right)}{\sum_{\{T_j\}} k_{je} \left(\sum_{ei} k_{ei} \right)} \tag{8.11}$$

and

$$\delta N_j = \frac{\sum_{\{T_j\}} \tilde{l}_{je} \left(\sum_{ei} \tilde{l}_{ei} \left(N_{ei} - N_j \right) \right)}{\sum_{\{T_j\}} \tilde{l}_{je} \left(\sum_{ei} \tilde{l}_{ei} \right)}, \tag{8.12}$$

each being an averaging process on U or N. Averaging processes have been exploited elsewhere [7],[9].

These algorithms clearly belong to the class of fluctuation-signal type schemes, even though the sum of the weights is zero and the iterations are non-conservative in the usual sense.

9 An Upwind Hybrid Method

As proposed in section 7 we may combine upwind iterations for **U** with least squares iterations for **N** in an obvious way by interleaving iterations for **U** from equation (8.3) with the least squares procedure for **N** from equations (8.6). In this way we may combine the benefits of a conservative and positive iteration for **U**, which follows the flow of information along characteristics, with an iteration for **N** which drives $\|\mathbf{\Phi}\|$ down to zero and thereby counteracts the effect of the null space.

We now consider weights based on physically based iterations together with their properties and link them to least squares iterations.

Recall that the fluctuation-signal mechanism (with appropriate weights) may be regarded as originating in a scheme for solving the time-dependent equation

$$u_t + div\,(u\underline{a}) = 0 \tag{9.1}$$

(cf. equation (2.2)), and hence if used as an iteration to solve equation (2.2) may be interpreted as proceeding to the steady state limit through

physical states. Such a physical approach to the limit suggests that the flow of information along characteristics should be respected and the initial approximation should consist of inflow conditions, which in turn suggests the use of upwind weights for U satisfying

$$\begin{aligned} w_{ei} &= 0 \quad k_{ei} \leq 0 \\ w_{ei} &\geq 0 \quad k_{ei} > 0. \end{aligned} \tag{9.2}$$

It is also desirable (although not essential) that the weights chosen should be such that the iteration for U is conservative. This means that appropriately scaled weights should satisfy

$$\sum w_{ei} = 1 \tag{9.3}$$

(which rules out least squares weights).

This type of iteration is associated with Multidimensional Upwinding methods [5] where by careful choice of the weights the schemes can be made both conservative and positive, as in the PSI scheme [6],[9].

Similar arguments can be applied to the weights γ (see below).

We may then combine such an iteration with a least squares iteration for N. In this way we obtain the benefits of the multidimensional upwind schemes as well as driving $\|\mathbf{\Phi}\|$down to zero, thus nullifying the effect of the null space.

We may go further by trying to incorporate upwinding into the iteration for N. In doing so we give up the formal minimisation of $\|\mathbf{\Phi}\|$ but obtain much faster convergence to a very similar optimal grid.

10 Upwind Least Squares Methods

The least squares approach embeds the original equation in a higher order equation. The correct solution is picked out from the larger set of solutions by an outflow condition which is the original differential equation applied at the outflow boundary. It may be therefore be argued that the weights should still exhibit an upwind bias.

One way of achieving such a bias is to carry out the minimisation of $\|\mathbf{\Phi}\|$ over only *downwind* nodal values and admit temporary discontinuities in U. The updates resulting from the minimisation still reduce $\|\mathbf{\Phi}\|$ but at the expense of generating discontinuities. This step may be followed by a

projection step which resets all upwind values of U in a cell in such a way as to restore continuity of U. The two steps are then repeated until convergence is achieved. The second step is not a descent step and will not reduce $\|\mathbf{\Phi}\|$ in general. At convergence we nevertheless obtain a continuous U which minimises $\|\mathbf{\Phi}\|$ because the gradient is zero.

The algorithm has a strong upwind bias which reflects the nature of the original problem and its dependence on characteristics. In fact the second of the two steps is automatically implied if the updates in the first step are carried out in the usual least squares manner but with upwinded updates suppressed. With an appropriate scaling the first step is then equivalent to the LDA scheme of Multidimensional Upwinding [2],[11].

The generalisation to adaptive meshes is straightforward and is again motivated by the flow of information. The norm $\|\mathbf{\Phi}\|$ is minimised over only *downwind* values of N and when the local updates are carried out N becomes discontinuous at the nodes. The projection step then resets all upwind N values in a cell so as to make N continuous again. At convergence we obtain a continuous N which has driven $\|\mathbf{\Phi}\|$ even further down towards zero.

The method may be called Adaptive Discontinuous Least Squares (ADLS).

As in the previous section this procedure for N may be interleaved with iterations from a standard upwinding scheme for U, such as PSI, providing an algorithm which takes full advantage of the hyperbolic nature of the problem as well as speeding up convergence and counteracting the effect of the null space.

11 Numerical Results

The canonical result for the unified least squares method is due to Phil Roe in [2]. The problem is that of the circular advection equation,

$$yu_x - xu_y = 0, \tag{11.1}$$

in a rectangular region $|x| < 1, 0 < y < 1$ with initial data $u = 0$ except for $u = 1$ at two adjacent gridpoints on the inflow side. The method is to minimise the residual

$$F = \sum_{cells} \frac{\Phi^2}{S} \tag{11.2}$$

over the nodal values and nodal coordinates. The iteration is performed using steepest descent least squares (for both the solution and the grid) and the

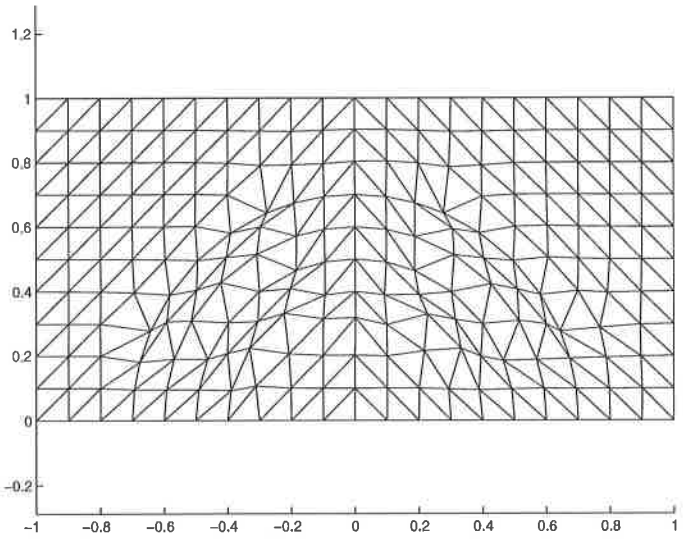

Figure 5: Resulting grid when using steepest descent least squares.

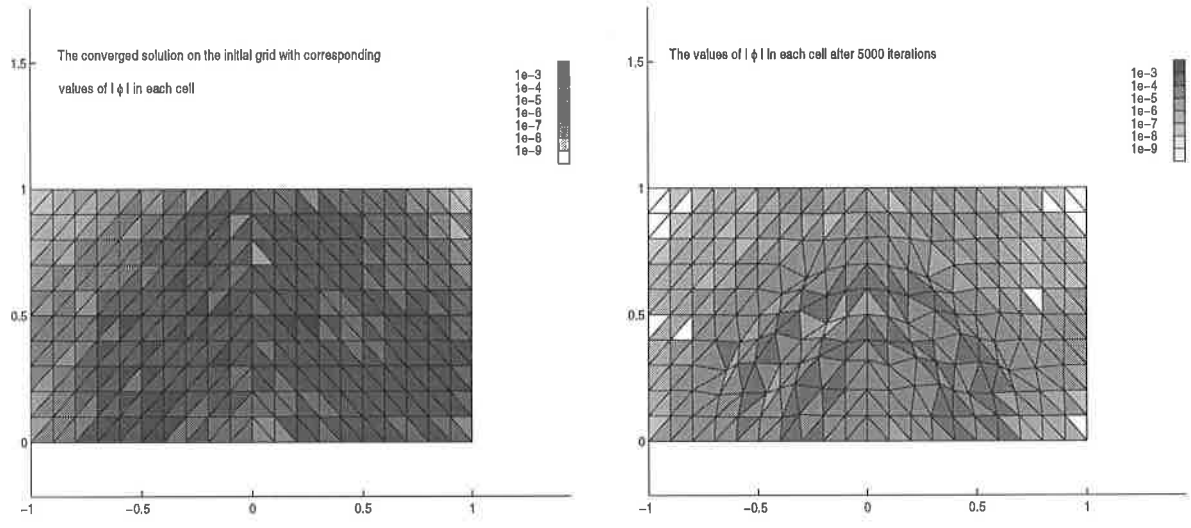

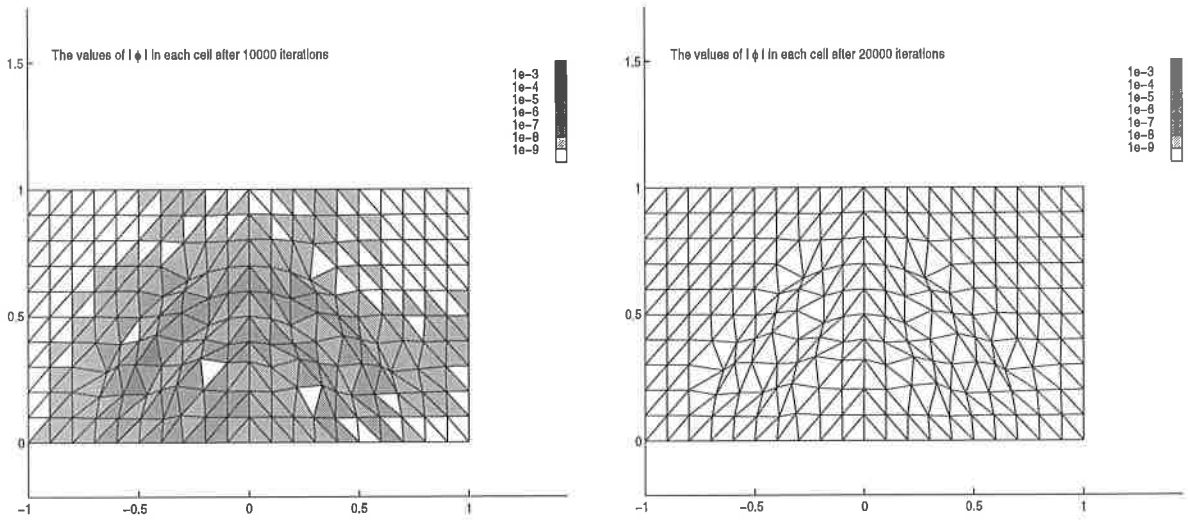

Figure 6: Results using steepest descent least squares.

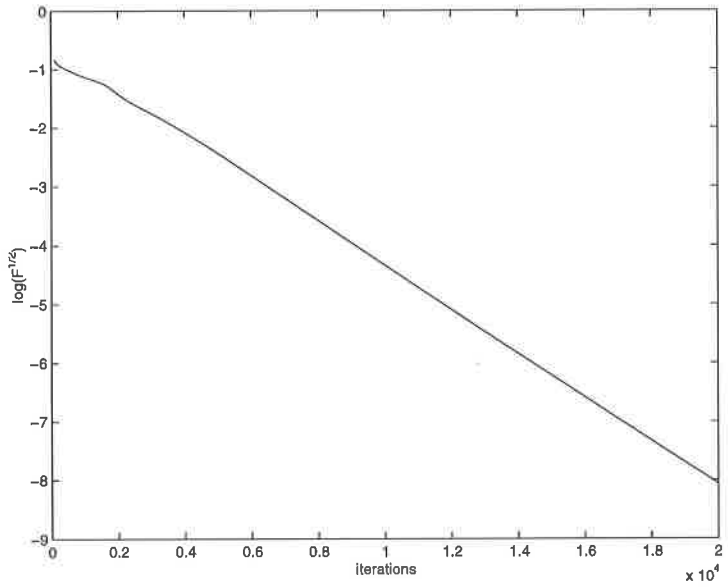

Figure 7: Convergence history when using steepest descent least squares.

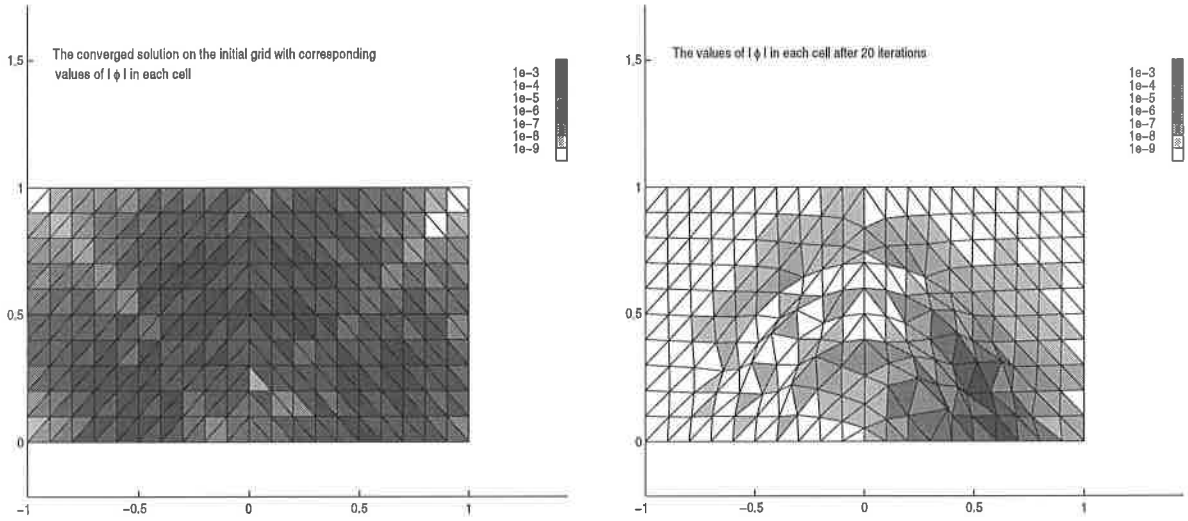

result is shown in fig. 3. In [2] the comparison between this result and that on a fixed grid is shown via graphs of the outflow profile. A different comparison may be made by shading the cells by the value of the local residual ($||\mathbf{\Phi}||$). In fig. 4 this shading is shown on grid plots for both the fixed and optimal grid solutions, as well as at two stages during the iteration, demonstrating the way in which the grid movement capability drives the residual down to very low values. Fig. 5 shows the corresponding convergence profile.

One of the drawbacks of the method is slow convergence. This is likely to be partly due to the way in which the least squares method updates upwind nodes as well as downwind nodes and partly due to lack of conservation. The iteration may be considerably accelerated by changing to the upwind least squares method of the previous section (for both the solution and the grid). However we find that some grid smoothing is needed. At the end of a period of alternately interleaving solution and node iterations the grid is subjected to the simple smoothing

$$\mathbf{X}_j^{new} = \frac{1}{N} \sum_{ji=1}^{N} \mathbf{X}_{ji} \tag{11.3}$$

where ji goes round the N outer nodes of the patch of cells surrounding node j, unless this results in mesh tangling. The result is much faster convergence to the same solution.

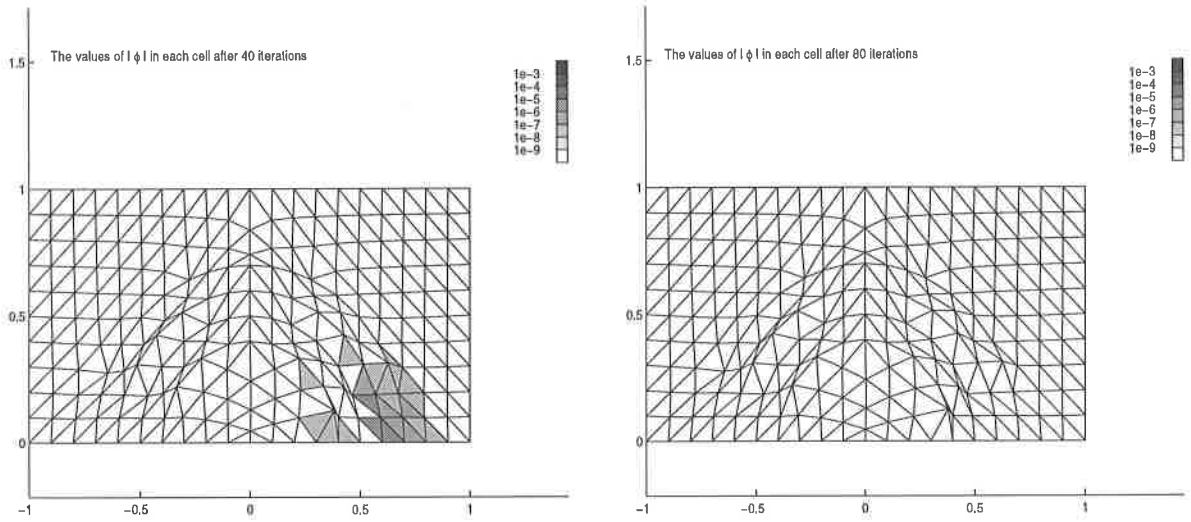

Figure 8: Results using upwind least squares.

In figure 6, starting from the fixed grid solution, we show grid plots after 0,20,40 and 80 iterations, shaded by the value of $\|\Phi\|$, and in figure 7 the corresponding convergence history.

12 Conclusion

In this paper difficulties experienced with fluctuation distribution methods on fixed unstructured grids in generating zero fluctuations/residuals has been addressed by including the mesh locations as variables. This allows the grid to adjust in order to drive the least squares residual of the fluctuation down closer to zero. The null space invoked by fixed grid methods is counteracted by the extra degrees of freedom provided by the moving nodes.

For a scalar advection problem in 2-D the procedure may be used in association with least squares minimisation of the average residual, giving a unified scheme for the solution and the grid, as in [2]. The resulting scheme is an approximate method of characteristics on a triangular grid. The nodes need only move perpendicular to the characteristics to provide the desired effect.

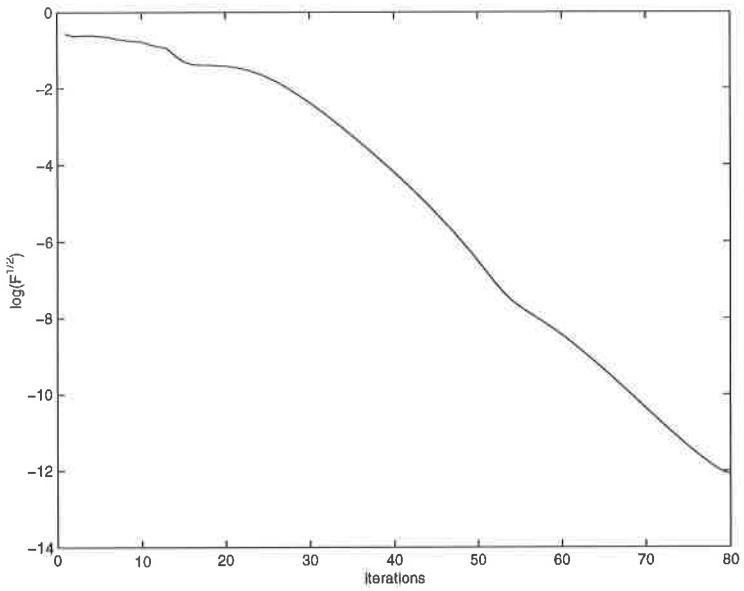

Figure 9: Convergence history when using upwind least squares.

The argument still holds when least squares is used only for the grid, with a more standard, physically based, scheme such as the PSI scheme used for the solution.

Iterative methods are discussed for the solution of the systems of equations which arise.

A hybrid multidimensional upwinding-least squares method is discussed and an interpretation of an upwind least squares iteration is given.

The discussion is restricted to a class of scalar advection equations in two dimensions but is also applicable to three dimensions. For systems of equations, where there is no single family of characteristics, the approach must rely on mesh movement in the mean.

13 Acknowledgements

The authors have benefitted greatly from discussions with Phil Roe, Yves Tourigny, Matthew Hubbard and Paul Houston.

14 References

[1] P.L.Roe (1983). Fluctuation and Signals: a framework for Numerical Evolution Problems. In Proceedings of IMA Conference on Numerical Methods for Fluid Dynamics, Reading, UK March 1982 (Morton and Baines (eds.)), p1, Academic Press.

[2] P.L.Roe (1996). Compounded of Many Simples, in Proceedings of Workshop on Barriers and Challenges in CFD, ICASE, NASA Langley, August 1996, (Ventakrishnan, Salas and Chakravarthy (eds.)), p241, Kluwer, 1998.

[3] Y.Tourigny and M.J.Baines (1997). Analysis of an Algorithm for Generating Locally Optimal Meshes for L_2 Approximation by Discontinuous Piecewise Polynomials, Math. Comp., 66,623-650.

[4] Y.Tourigny and F.Hulsemann (1997). A New Moving Mesh Algorithm for the Finite Element Solution of Variational Problems, SIAM.J.Num.An.(to appear).

[5] M.J.Baines (1997). On Variational Techniques and Least Squares Methods with Adjustable Nodes. Numerical Analysis Report 2/97, Department of Mathematics, University of Reading.

[6] H.Deconinck, P.L.Roe and R.Struijs (1993). A Multidimensional Generalisation of Roe's Flux Difference Splitter for the Euler Equations. Computers and Fluids, 22, 215.

[7] M.E.Hubbard (1994). Multidimensional Upwinding. PhD thesis, Department of Mathematics, University of Reading.

[8] M.J.Baines (1997). A Note on Duality for a Scalar Hyperbolic Equation. Numerical Analysis Report 8/97, Department of Mathematics, University of Reading.

[9] M.J.Baines and M.E.Hubbard (1998). Multidimensional Upwinding and Grid Adaptation. In Numerical Methods for Wave Propagation Problems (E.F.Toro and J.F.Clarke (eds.)), Kluwer.

[10] N.R.C.Birkett and M.Rudgyard (1998). In Proceedings of 1998 ICFD Conference on Numerical Methods for Fluid Dynamics (M.J.Baines (ed.)), ICFD, Oxford University Computing Laboratory.